# Staphylococcal Enterotoxin A Is Encoded by Phage

Abstract. *The gene for staphylococcal enterotoxin A (*entA*), in two wild-type strains, is carried by related temperate bacteriophages. Hybridization analysis of DNA from* entA*-converting phage PS42-D and its bacterial host suggests that this phage integrates into the bacterial chromosome by circularization and reciprocal crossover (the Campbell model) and that the* entA *gene is located near the phage attachment site. DNA from three of eight staphylococcal strains that did not produce enterotoxin A and seven wild-type enterotoxin A–producing (EntA$^+$) strains had extensive homology to the* entA*-converting phage PS42-D DNA, although there was a high degree of restriction-fragment length polymorphisms. At least one EntA$^+$ strain did not produce detectable viable phage after induction. These data indicate that a polymorphic family of* Staphylococcus aureus *phages (some of which may be defective) can carry the* entA *gene.*

MARSHA J. BETLEY
JOHN J. MEKALANOS
*Department of Microbiology and Molecular Genetics, Harvard Medical School, Boston, Massachusetts 02115*

Staphylococcal enterotoxins are the causative agents of staphylococcal food poisoning (*1*). The enterotoxins are classified into five serologic groups (A, B, C, D, and E), but have similar biological and structural properties (*1*).

The staphylococcal enterotoxin A (SEA) gene (*entA*) has been mapped between the purine (*pur*) and isoleucine-valine (*ilv*) markers in 24 *Staphylococcus aureus* strains; but, in five SEA-producing (EntA$^+$) strains, the *entA* gene was in none of the analyzable chromosomal linkage groups or on detectable plasmid DNA (*2*, *3*). DNA hybridization analysis of EntA$^+$ strains with a probe containing a cloned *entA* gene confirmed the results of genetic experiments that had shown different chromosomal locations for the *entA* gene among *S. aureus* strains (*4*). In addition, the *entA* gene was located on an element that was at least 8 kilobases (kb) in length. This element was absent in some EntA$^-$ strains, although DNA from a few EntA$^-$ strains has some homology to the *entA*-element DNA (*4*).

The *S. aureus* strain PS42-D (EntA$^+$) has been reported to contain a prophage with the EntA$^+$-associated phenotype, although no EntA$^+$-associated phages were detected in two other EntA$^+$ strains (*5*, *6*). We now report that the *entA* gene is associated with a phage in all strains examined and that these *entA*-converting phages show heterogeneity in restriction endonuclease analysis.

Initially, we confirmed earlier observations that a phage derived from *S. aureus* PS42-D could convert a nontoxinogenic strain of *S. aureus* to EntA$^+$ (*5*, *6*). An ultraviolet irradiation (UV)–induced phage lysate from PS42-D was used to infect ISP456 (EntA$^-$) (*7*). Each of six purified lysogenized bacterial strains was EntA$^+$ as determined by antigen-antibody reactions in agar (*3*) and contained a UV-inducible prophage that formed plaques on ISP456 but not on PS42-D. This phage was shown to carry the *entA* structural gene rather than a regulatory gene by means of Southern blot hybridization with pMJB3, a recombinant pBR322 plasmid that contains the *entA* gene of strain MJB106 in an 8-kb insert (*4*). The phage donor strain (PS42-D) and the lysogenized strains contained the *entA* gene and surrounding sequences, while the indicator strain (ISP456) lacked this DNA (Fig. 1). The hybridization patterns were the same among the EntA$^+$ strains PS42-D, MJB233, and FRI337, except for the length polymorphisms of the largest fragments.

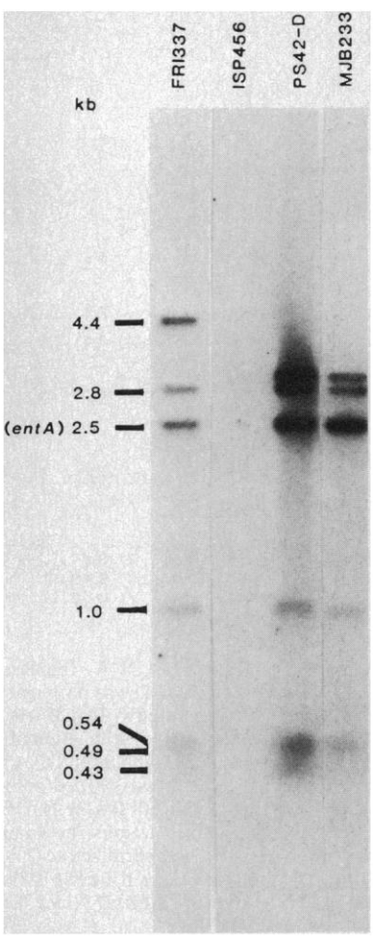


Fig. 1. Southern blots of whole cell DNA from phage donor, indicator, and lysogenized *S. aureus* strains. MJB233 is a representative of one of six isolates of ISP456 lysogenized with phage from PS42-D. The probe was $^{32}$P-labeled pMJB3, a pBR322 recombinant clone that has the *entA* gene of a derivative of FRI337 (MJB106) (*4*). Hind III digests of DNA were analyzed by electrophoresis on a 1.2 percent agarose gel (*4*); the DNA was transferred onto nitrocellulose (*22*) and hybridized to nick-translated $^{32}$P-labeled pMJB3 (*23*). Whole cell DNA was prepared as described (*24*).

Phage PS42-D contains a linear DNA molecule (Fig. 2A) that has cohesive ends. A fragment that was the sum of the end fragments was visible in the ethidium bromide–stained agarose gels of each restriction digest of phage DNA (for example, Fig. 2B, lane 1). Heating the restriction digests for 20 minutes at 68°C prior to electrophoresis resulted in a decrease in the amount of the annealed end fragments and an increase in the amount of each of the end fragments.

The location of the *entA* gene in phage PS42-D DNA (Fig. 2A) was determined by analyzing Southern blots of restriction digests of phage DNA hybridized to pMJB38, a pBR322 recombinant plasmid that contains a 623–base pair fragment derived from DNA internal to the *entA* structural gene (*8*) (Fig. 2B, lane 3). With this probe, we have also shown that the *entA* gene is encoded on a 2.5-kb Hind III fragment in bacterial strains FRI337, PS42-D, and MJB233.

The data (Fig. 2B) suggest that the DNA preparation from the lysogenized strain MJB233 contains both linear phage DNA and prophage DNA that has integrated into bacterial DNA by circularization and reciprocal crossover (the Campbell model) (Fig. 2B) (*9*). The same set of restriction fragments was observed in phage PS42-D DNA as in MJB233 DNA that had been digested with Sal AI and Mlu I and then hybridized to $^{32}$P-labeled phage PS42-D DNA; this indicates that MJB233 DNA preparations contain linear phage DNA molecules (Fig. 2B, lanes 1, 5, and 6). In order for the phage DNA to integrate, it apparently circularizes by fusing the 2.5- and 10-kb cohesive end fragments to form the 12.5-kb fragment in the Sal AI–Mlu I digest. This fusion fragment was visible in phage preparations because the linear phage DNA molecules do anneal and also occurred in whole cell lysogenized

bacterial DNA (Fig. 2B, lanes 5 and 6). In addition, MJB233 preparations contained two fragments that were not observed in phage PS42-D; these fragments contain the junctions between the prophage and bacterial DNA (Fig. 2B, lanes 5 and 6).

The *entA* gene was found at one of these prophage-bacterial DNA junction fragments by examination of Southern blots of MJB233 probed with the internal fragment of the *entA* gene (Fig. 2B, lanes 4 and 6, contain a representative blot). This localization was also observed in nine other restriction enzyme digests of whole cell DNA from MJB233 (*10*). Therefore, the phage attachment site must be very near the *entA* gene. MJB233 has a second *entA*-hybridizing fragment that corresponds in size to the *entA* fragment found in the linear phage DNA (Fig. 2, lane 4). Therefore, the whole cell DNA preparation appears to contain both linear and prophage DNA molecules. The linear DNA may represent intracellular replicative intermediates or cell-adsorbed phage particles that were derived from spontaneous induction of a fraction of these lysogenic cells.

Next, we investigated the relationship between phage PS42-D and EntA$^+$ or EntA$^-$ *S. aureus* strains. Five of eight EntA$^-$ strains did not hybridize to phage PS42-D DNA (Fig. 3, lanes K to R), although two of these EntA$^-$ strains, ISP546 and RN450, are related (*3*). In contrast, all EntA$^+$ strains contained a substantial amount of DNA homologous to phage PS42-D DNA although differences were observed (Fig. 3, lanes A to J). For example, blots of these EntA$^+$ strains have different subsets of Hind III fragments in common with each other. These results suggest that the *entA* genes in these strains are associated with a family of phages, rather than with one particular phage. Similar polymorphisms were seen with Hpa I and Sal AI–Pst I restriction endonucleases digests.

To prove that phage PS42-D is not the only viable *entA*-encoding phage, we isolated an *entA*-converting phage (FRI337-1) from bacterial strain FRI337. RN450, an EntA$^-$ strain, was converted to EntA$^+$ after being lysogenized with this phage. The Hind III digest of DNA from FRI337-1 was compared to DNA of plasmid pMJB3, which contains an insert from a derivative of FRI337 and encodes *entA* on the 2.5-kb Hind III fragment (*4*). The phage and plasmid had common sequences that included the *entA*-containing fragment (*11*).

The *entA*-encoding phages must have a preferred chromosomal attachment site in the *pur-ilv* region, because the *entA* gene maps in this region in 24 of 29 EntA$^+$ strains (*2*, *3*). FRI337, FRI371, and FRI1019 are three wild-type bacterial strains whose *entA* genes are linked to the *pur-ilv* region (*2*, *3*) (Fig. 3, lanes B, D, and E). FRI610, FRI708, FRI1000, and FRI710 are wild-type strains whose functional *entA* genes are unlinked to the *pur-ilv* markers (*3*) (Fig. 3, lanes F to I). The latter four strains also contain DNA in the *pur-ilv* region that is homologous to pMJB3 (*4*) and thus to phage FRI337-1. Moreover, these two regions of phage-DNA homology (the *pur-ilv* region and the region containing the functional *entA* gene) in FRI710 have been separated by transformation to form MJB234 (EntA$^+$) and MJB164 (EntA$^-$) (Fig. 3, lanes J and K) (*12*). These results suggest that some strains contain more than one prophage related to *entA*-converting phages and that these prophages integrated at different locations within a strain.

ISP484 carries a prophage related to the *entA*-converting phages (Fig. 3, lane M), but this prophage was shown to lack the *entA* gene by the absence of hybridization to the internal fragment of the *entA* gene in pMJB38. Two other EntA$^-$ strains that have homology to *entA*-converting phage DNA are MJB164 and FRI776 (Fig. 3, lanes K and O).

Some *entA* genes are apparently asso-

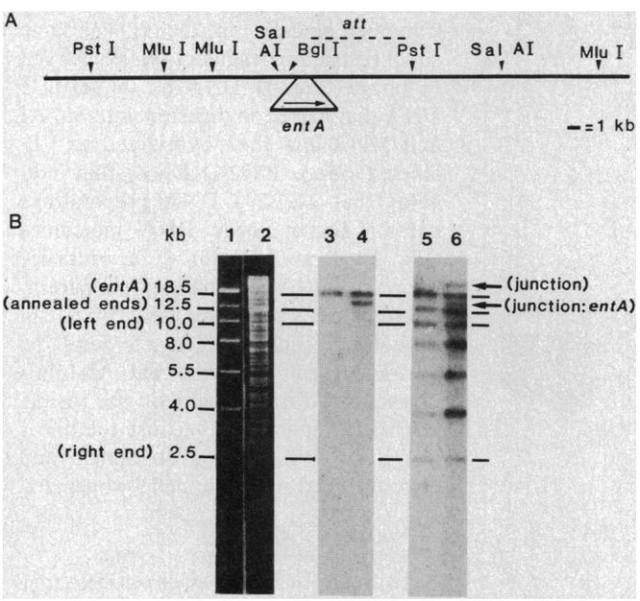


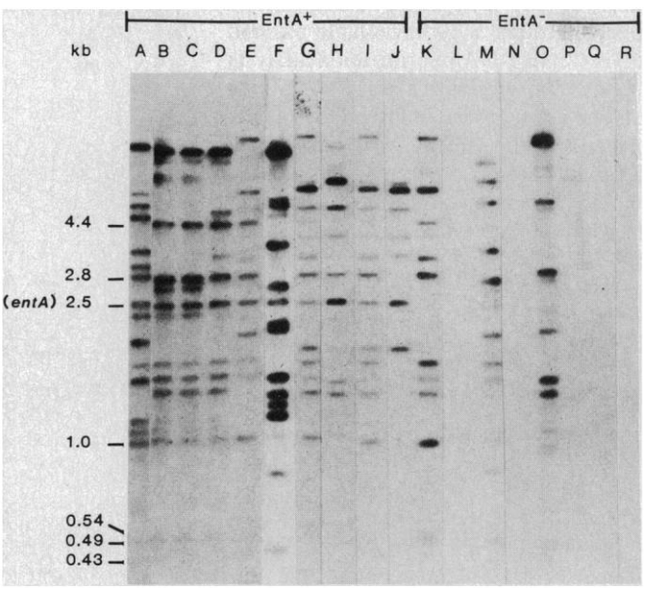


Fig. 2 (left). (A) Restriction endonuclease cleavage-site map of phage PS42-D DNA. The dashed line indicates the region that contains the phage attachment site (*att*), although the precise location is not known. Phage PS42-D was propagated on ISP456 in a soft agar overlay as described (*25*) except agarose was used in the overlay instead of agar. Phages were harvested in 50 m*M* tris hydroxymethylaminomethane, 10 m*M* NaCl, 4 m*M* $MgSO_4$, and 0.12 percent gelatin (*p*H 8) and their DNA was isolated (*26*). (B) Hybridization of phage PS42-D DNA and whole cell DNA from lysogenic bacterial strain MJB233. Phage PS42-D (lanes 1, 3, and 5) and MJB233 whole cell DNA's (lanes 2, 4, and 6) were codigested with Sal AI and Mlu I. An ethidium bromide–stained 0.9 percent agarose gel (lanes 1 and 2) was blotted onto a nitrocellulose filter and hybridized to $^{32}$P-labeled pMJB38 (lanes 3 and 4). The first probe was then removed by treatment with 0.02*M* NaOH, and the test DNA's were rehybridized with $^{32}$P-labeled phage PS42-D DNA (lanes 5 and 6). Left and right refer to the orientations shown in (A). Fig. 3 (right). Hybridization of whole cell DNA from EntA$^+$ and EntA$^-$ *S. aureus* strains digested with Hind III and hybridized to $^{32}$P-labeled phage PS42-D DNA. DNA is from MJB233 (lane A), FRI337 (lane B), MJB106 (lane C), FRI371 (lane D), MJB1019 (lane E), FRI610 (lane F), FRI708 (lane G), FRI1000 (lane H), FRI710 (lane I), MJB234 (lane J), MJB164 (lane K), RN450 (lane L), ISP484 (lane M), FRI777 (lane N), FRI776 (lane O), FRI184 (lane P), ISP546 (lane Q), and ISP456 (lane R).

ciated with either defective phages or phages altered in host range. We were unable to isolate any plaque-forming units from the EntA$^+$ strain MJB234, which carries DNA homologous to phage PS42-D. This may be the reason that *entA*-converting phages could not be identified in two strains previously examined (*5, 6*).

Our results show that a gene for a *S. aureus* toxin is correlated with phage DNA in all strains examined. Although Blair and Carr (*13*) demonstrated that the ability to produce α-toxin could be acquired by two of three nontoxinogenic strains after lysogenization by the phage L2043, this phage may encode either a regulatory or a structural gene for α-toxin. However, for a different strain, no biochemical evidence for prophage involvement with α-toxin synthesis was obtained (*14*). The significance of the observation (*15*) that *S. aureus* strains associated with toxic shock syndrome may have a common temperate phage is unclear; Kreiswirth *et al.* (*16*) were unable to demonstrate an association between the presence of phage and toxic shock syndrome exotoxin production. These conflicting observations may be due to the respective toxin-converting phages being highly polymorphic in properties such as viability and host range.

There are examples of other bacterial species carrying phages that determine toxin production. The structural genes for diphtheria toxin (*17*), erythrogenic toxin of *Streptococcus pyogenes* (*18*), the structural or regulatory genes of botulinum toxins $C_1$ and D (*19*), and the shiga-like toxin of *Escherichia coli* (*20*) are all encoded by temperate phage. How nontoxinogenic phages initially acquired toxin genes is unknown. The diphtheria toxin gene (*21*) and the *entA* gene are both located near the phage attachment site on the genomes of their respective converting phages (Fig. 2). Perhaps the *entA*-converting phage formed as a result of an imprecise excision event between a chromosomal enterotoxin gene and a closely inserted nontoxinogenic prophage, as proposed by Laird and Groman for diphtheria toxin (*21*). Consistent with this hypothesis is our observation that there exist phages that lack the *entA* gene but are related to the *entA*-converting phages. Recombination between these various types of phages may provide a mechanism for the formation of new *entA*-converting phages that have increased host range, or possibly enterotoxin genes with different serological, structural, and biological properties.


**References and Notes**

1. M. S. Bergdoll, in *Food-borne Infections and Intoxications*, H. Riemann and F. L. Bryan, Eds. (Academic Press, New York, 1979), pp. 443–493.
2. P. A. Pattee and B. A. Glatz, *Appl. Environ. Microbiol.* **39**, 186 (1980).
3. D. H. Mallone, B. A. Glatz, P. A. Pattee, *ibid.* **43**, 397 (1982).
4. M. J. Betley *et al.*, *Proc. Natl. Acad. Sci. U.S.A.* **81**, 5197 (1984).
5. E. P. Casman, *Ann. N.Y. Acad. Sci.* **128**, 124 (1965).
6. A. W. Jarvis and R. C. Lawrence, *Infect. Immun.* **4**, 110 (1971).
7. Strain ISP456 is the restriction-deficient mutant 80 CR3 described by E. E. Stobberingh and K. C. Winkler [*J. Gen. Microbiol.* **99**, 359 (1977)].
8. The plasmid pMJB38 is a pBR322 recombinant plasmid that contains a 623-bp fragment derived from DNA internal to the *entA* structural gene as determined by sequence analysis.
9. A. M. Campell, *Adv. Genet.* **11**, 101 (1962).
10. Analysis of Southern blots with enzyme digests of whole cell DNA from MJB233 and PS42-D DNA that had been hybridized to $^{32}$P-labeled pMJB38 was consistent with the interpretation that whole cell DNA from MJB233 contained both linear and prophage DNA molecules and that the *entA* gene was located near one of the prophage-bacterial junctions. The DNA's were each digested with the following enzymes: Bgl I, Mlu I, Pst I, Sal AI, Bgl I–Mlu I, Bgl I–Pst I, Bgl I–Sal AI, Mlu I–Pst I, and Pst–Sal AI.
11. The phage FRI337-1 was shown to encode the *entA* gene on a 2.5-kb Hind III fragment by Southern blot hybridization with pMJB38 as probe.
12. MJB234 is an EntA$^+$ erythromycin-resistant (Erm$^r$) transformant of FRI710 (EntA$^+$, erythromycin-sensitive) whose relevant portion of the *pur-ilv* region is substituted with DNA from ISP546 (EntA$^-$ Erm$^r$). MJB164 (EntA$^-$; purine, isoleucine, and valine prototroph) is a transformant of ISP484 (EntA$^+$; purine, isoleucine, and valine auxotroph) that contains FRI710's *pur-ilv* region (*4*).
13. J. E. Blair and M. Carr, *J. Bacteriol.* **82**, 984 (1961).
14. C. W. Hendricks and R. A. Altenbern, *Can. J. Microbiol.* **14**, 1277 (1968).
15. S. C. Schutzer, V. A. Fischetti, J. B. Zabriskie, *Science* **220**, 316 (1983).
16. B. N. Kreiswirth *et al.*, *Nature (London)* **305**, 709 (1983).
17. L. Barksdale, L. Garmise, R. Rivera, *J. Bacteriol.* **81**, 527 (1967); J. Murphy, A. M. Pappenheimer, Jr., S. T. de Broms, *Proc. Natl. Acad. Sci. U.S.A.* **71**, 11 (1974).
18. J. B. Zabriskie, *J. Exp. Med.* **119**, 761 (1974); C. R. Weeks and J. J. Ferretti, *Infect. Immun.* **46**, 531 (1984).
19. K. Inoue and H. Iida, *C. Jpn. J. Microbiol.* **14**, 87 (1970); *Jpn. J. Med. Sci. Biol.* **24**, 53 (1971).
20. A. D. O'Brien *et al.*, *Science* **226**, 694 (1984).
21. R. K. Holmes, *J. Virol.* **19**, 195 (1976); W. Laird and N. Groman, *ibid.*, p. 208; *ibid.*, p. 228; R. K. Holmes and L. Barksdale, *ibid.* **3**, 586 (1969).
22. Modifications of the DNA-DNA hybridization procedure [E. Southern, *J. Mol. Biol.* **98**, 503 (1975)] have been described [J. J. Mekalanos, *Cell* **35**, 253 (1983)].
23. T. Maniatis, A. Jeffrey, D. G. Kleid, *Proc. Natl. Acad. Sci. U.S.A.* **72**, 1184 (1975).
24. M. L. Stahl and P. A. Pattee, *J. Bacteriol.* **154**, 395 (1983).
25. N. E. Thompson and P. A. Pattee, *ibid.* **148**, 294 (1981).
26. R. W. Davis, D. Botstein, J. R. Roth. *Advanced Bacterial Genetics—A Manual for Genetic Engineering* (Cold Spring Harbor Laboratory, Cold Spring Harbor, N.Y., 1980), pp. 109–111.


27. We thank G. A. Hancock, W. J. van Leeuwen, A. W. Jarvis, and P. A. Pattee for providing bacterial strains. Supported by a Damon Runyon–Walter Winchell Cancer Fund fellowship, DRG-733 (M.J.B.).

15 February 1985; accepted 15 May 1985


# Localized Control of Ligand Binding in Hemoglobin: Effect of Tertiary Structure on Picosecond Geminate Recombination


Abstract. *The picosecond geminate rebinding of molecular oxygen was monitored in a variety of different human, reptilian, and fish hemoglobins. The fast (100 to 200 picoseconds) component of the rebinding is highly sensitive to protein structure. Both proximal and distal perturbations of the heme affect this rebinding process. The rebinding yield for the fast process correlates with the frequency of the stretching motion of the iron–proximal histidine mode ($\nu_{Fe\text{-}His}$) observed in the transient Raman spectra of photodissociated ligated hemoglobins. The high-affinity R-state species exhibit the highest values for $\nu_{Fe\text{-}His}$ and the highest yields for fast rebinding, whereas low affinity R-state species and T-state species exhibit lower values of $\nu_{Fe\text{-}His}$ and correspondingly reduced yields for this geminate process. These findings link protein control of ligand binding with events at the heme.*



**J. M. Friedman**
**T. W. Scott***
**G. J. Fisanick**
*AT&T Bell Laboratories, Murray Hill, New Jersey 07974*
**S. R. Simon**
*Department of Biochemistry, State University of New York, Stony Brook 11794*
**E. W. Findsen**
**M. R. Ondrias**
*Department of Chemistry, University of New Mexico, Albuquerque 87106*
**V. W. Macdonald**
*Department of Hematology, Johns Hopkins Medical Center, Baltimore, Maryland 21205*


Hemoglobin (Hb) reactivity toward ligands such as $O_2$ or CO is characterized by macroscopic measurements of ligand binding ("on" rates) and ligand dissociation ("off" rates). These parameters of reactivity are highly responsive to protein structure. One acquires coarse control of the reactivity by changing the quaternary structure. The two well-defined quaternary structures of hemoglobin (*1, 2*), termed the R state and T state, exhibit, respectively, enhanced and reduced reactivity toward these ligands (*1*). Fine tuning of the reactivity can occur through solution-induced or spe-


*Present address: Corporate Research Science Laboratories, Exxon Research Laboratories, Annandale, N.J. 08801.